

Published in final edited form as:

*Stem Cells Dev.* 2008 December ; 17(6): 1023–1029. doi:10.1089/scd.2008.0091.

## In Vivo Imaging of Embryonic Stem Cells Reveals Patterns of Survival and Immune Rejection Following Transplantation

Rutger-Jan Swijnenburg<sup>1,5</sup>, Sonja Schrepfer<sup>1</sup>, Feng Cao<sup>2</sup>, Jeremy I. Pearl<sup>1</sup>, Xiaoyan Xie<sup>2</sup>, Andrew J. Connolly<sup>3</sup>, Robert C. Robbins<sup>1</sup>, and Joseph C. Wu<sup>2,4</sup>

<sup>1</sup> Department of Cardiothoracic Surgery, Stanford University School of Medicine, Stanford, California <sup>2</sup> Molecular Imaging Program at Stanford (MIPS), Stanford University School of Medicine, Stanford, California <sup>3</sup> Department of Pathology, Stanford University School of Medicine, Stanford, California <sup>4</sup> Department of Medicine, Division of Cardiology, Stanford University School of Medicine, Stanford, California <sup>5</sup> Department of Surgery, Leiden University Medical Center, Leiden, The Netherlands

### Abstract

Embryonic stem cell (ESC)-based transplantation is considered a promising novel therapy for a variety of diseases. This is bolstered by the suggested immune-privileged properties of ESCs. In this study, we used in vivo bioluminescent imaging (BLI) to non-invasively track the fate of transplanted murine ESCs (mESCs), which are stably transduced with a double fusion reporter gene consisting of firefly luciferase (FLuc) and enhanced green fluorescent protein (eGFP). Following syngeneic intramuscular transplantation of  $1 \times 10^6$  mESCs, the cells survived and differentiated into teratomas. In contrast, allogeneic mESC transplants were infiltrated by a variety of inflammatory cells, leading to rejection within 28 days. Acceleration of rejection was observed when mESCs were allotransplanted following prior sensitization of the host. Finally, we demonstrate that the mESC derivatives were more rapidly rejected compared to undifferentiated mESCs. These data show that mESCs do not retain immune-privileged properties in vivo and are subject to immunological rejection as assessed by novel molecular imaging approaches.

Embryonic stem cell (ESC)-based transplantation therapies have significant potential for treating a broad spectrum of human diseases either by replacement or by regeneration of lost or damaged tissues [1]. ESCs are pluripotent and have the capacity to differentiate into multiple adult cell types in vitro, such as cardiomyocytes [2], pancreatic islet cells [3], and neurons [4]. These ESC derivatives have demonstrated therapeutic potential in vivo [5]. One potential benefit of ESC-based transplantation over adult cells is their suggested immune-privileged properties [6]. Human (h) and murine (m) ESCs have been shown to express low levels of major histocompatibility (MHC) antigens [7,8]. Previous studies have reported that both mESCs [9] and hESCs [10] are capable of inhibiting allogeneic T-cell proliferation in vitro. Furthermore, mESCs have been shown to evade immune recognition and survive in immunocompetent rats [11] and sheep [12] for many weeks after transplantation. Nevertheless, our group and others have found that mESCs transplanted into allogeneic mouse hearts can elicit local graft infiltration of inflammatory cells resulting in rejection [13,14]. Similarly, other reports have questioned the alleged immune privilege of mESCs following xenotransplantation into immunocompetent baboons [15].

Clearly, the extent to which immunologic rejection of ESCs and/or ESC derivatives occurs following allogeneic transplantation is a crucial question that has not yet been clarified. The results of aforementioned studies were primarily based on immunohistological evaluation, which provide only a “snapshot” representation rather than a comprehensive picture of cell survival over time [16]. Such limited techniques may partly contribute to the conflicting observations of mESC survival in allogeneic or xenogeneic hosts. To address these limitations, we have previously validated *in vivo* bioluminescent imaging (BLI) to be a reliable technique for assessing engraftment and survival of mESCs following transplantation *in vivo* [17]. An important advantage in using BLI to track cell transplantation is that the expression of the firefly luciferase (Fluc) reporter gene, which is integrated into the DNA of the transplanted cells, is expressed only by living cells, making it a highly accurate tool for following cell graft rejection in the living subject [18]. We have previously shown that the transduction of mESCs with reporter genes that allow *in vivo* tracking does not alter cellular viability and their ability to differentiate into cells of all three germ layers [19,20]. To further delineate the novel field of ESC transplantation immunobiology, we used *in vivo* BLI to visualize patterns of survival and rejection of mESCs following transplantation across histocompatibility barriers.

To track the mESCs *in vivo* by BLI as well as *ex vivo* by immunohistochemistry, a double fusion (DF) reporter gene construct carrying Fluc and enhanced green fluorescent protein (eGFP) driven by a constitutive ubiquitin promoter (pUB) was transduced into undifferentiated mESCs (D3 cell line, derived from the 129/Sv mouse strain), using a self-inactivating (SIN) lentiviral vector (Fig. 1A), as described previously [20]. After transduction, mESCs robustly expressed Fluc (Fig. 1B) and eGFP (Fig. 1C). In agreement with the previous reports [9,21], flow cytometric analysis showed the expression of pluripotency marker SSEA-1 and minimal expression of H-2k<sup>b</sup> MHC class I (MHC-I) or I-A<sup>b</sup> MHC class II (MHC-II) antigens on undifferentiated mESCs. In contrast, mESC-derived teratoma cells (mES-TCs) isolated from 6-week-old surgically explanted teratomas by a 2-h enzymatic digestion in Collagenase D (2 mg/mL in RPMI medium) clearly expressed both MHC-I and MHC-II antigens (Fig. 1D). In culture, mES-TCs displayed a heterogeneous single cell morphology, as opposed to mESCs, which grow in tight clusters (Fig. 1E).

Transduced mESCs ( $1 \times 10^6$ ) were transplanted by direct injection into the gastrocnemius muscle of syngeneic (129/Sv, H-2k<sup>b</sup>,  $n = 8$ ) and allogeneic (BALB/c, H-2k<sup>d</sup>,  $n = 8$ ) recipient mice, after which BLI was performed weekly. The BLI protocol involved intraperitoneal administration of the d-Luciferin reporter probe at a dose of 375 mg/kg body weight and imaging was performed using the Xenogen *In Vivo* Imaging System as described previously [17]. Clearly, impaired survival of mESCs in the allogeneic recipients was observed as compared to the syngeneic animals, reaching statistical significance at day 14 after transplantation (BLI signal: 129/Sv  $9.00 \pm 0.57$  vs. BALB/c  $7.54 \pm 0.99$  Log<sup>[photons/s]</sup>;  $p < 0.01$  by *t*-test). (Fig. 2A and B). By 28 days, BLI signal in the allogeneic recipients had decreased to background levels, whereas signal in the syngeneic recipients continued to increase. These results suggest alloantigen-specific rejection of the transplanted mESCs. At 28 days following transplantation, gastrocnemius muscles were surgically explanted. In syngeneic recipients, intramuscular tumors could be observed, whereas the shape of the allogeneic recipient muscles appeared normal (Fig. 2C). Differentiated structures originating from all three germ layers could be demonstrated by H&E staining in the syngeneic muscles, indicating teratoma formation. Correlating with our findings using BLI, no teratoma formation and/or signs of surviving mESCs could be found in the allogeneic muscles (Fig. 2C).

We next investigated the local immune response elicited by mESCs in a second group of allogeneic BALB/c and syngeneic 129/Sv mice ( $n = 8$  per group). At 10 days following transplantation, the muscles of these mice were explanted and investigated for graft-infiltrating cells. Immunofluorescent staining of allogeneic muscle sections demonstrated massive

infiltration of CD45<sup>+</sup> inflammatory cells surrounding the eGFP<sup>+</sup> mESC grafts (Fig. 2D). Quantification and further characterization of graft-infiltrating cells was carried out by enzymatic digestion (2 h in 2 mg/mL collagenase D in RPMI medium) of the explanted muscles followed by FACS analysis. Live cells were gated out from debris and further analyzed for the expression of a panel of hematopoietic cell surface markers. Comparison of the syngeneic to the allogeneic mESC recipient muscles confirmed severe infiltration of various types of immune cells involved in both adaptive and innate types of immunity (Fig. 2E). At this time-point, both the CD3<sup>+</sup> cells (total T-cell population) and CD8<sup>+</sup> cells (cytotoxic T-cells) were present at a significantly higher frequency in allogeneic versus syngeneic recipients ( $p < 0.05$  by *t*-test), suggesting a prominent role for T-cell-mediated immunity in mESC rejection.

To investigate whether mESCs could induce immunologic memory, we next performed infusion of  $1 \times 10^6$  nontransduced D3 mESCs or  $1 \times 10^6$  irradiated (3,000 rad) 129/Sv splenocytes (as control) into the tail vein of allogeneic BALB/c recipients ( $n = 4$  and 5 per group, respectively). Four weeks later, these same mice received intramuscular transplantation with the same number of transduced mESCs and cell survival was quantified using longitudinal BLI. Accelerated BLI signal loss was observed in both groups, with BLI signal reaching background levels as soon as post-transplant day 4 (control group) and day 7 (mESC group) (Fig. 3A and B). These findings confirm that a donor (129/Sv)-specific adaptive immune response is generated against transplanted mESCs.

Clinical ESC-based transplantation protocols will require differentiation of the donor cells into the desired cell type before transplantation, due to the risk of teratoma formation following transplantation of undifferentiated ESCs [13]. Therefore, we thought that it would be relevant to study the survival of mESC derivatives following allotransplantation. A group of BALB/c mice ( $n = 5$ ) was injected with  $1 \times 10^6$  mES-TCs and longitudinal BLI was performed. In comparison with undifferentiated mESCs, the BLI signal displayed a similar pattern up until 7 days following transplantation (Fig. 4A and B). However, BLI signal in the mES-TC animals decreased substantially by day 10 (mESC  $7.74 \pm 0.58$  vs. mES-TC  $5.46 \pm 0.17$  Log<sup>[photons/s]</sup>;  $p < 0.01$  by *t*-test) and reached background levels at day 14. These results show that differentiated mESCs have impaired survival capacity as compared to undifferentiated mESCs when transplanted over histocompatibility barriers.

In a recent report, higher numbers of transplanted undifferentiated mESCs ( $5 \times 10^6$ – $20 \times 10^6$ ) were shown capable of survival and formation of teratoma in allogeneic recipients [22]. Similarly, in this study we found that when  $10 \times 10^6$  mESCs were transplanted into allogeneic BALB/c recipient muscles, BLI signal could be followed out beyond 28 days following transplantation in 2 out of 10 animals (20%) and intramuscular teratomas could be observed in these two animals. However, when mESCs were allowed to differentiate for 14 days in vitro prior to transplantation,  $10 \times 10^6$  cells were rejected by 10 out of 10 animals (100%) (data not shown).

Undifferentiated mESCs have been reported to possess immune-privileged properties, which has been attributed to the low expression of MHC molecules [21], expression of perforin-deactivating Serpin-6 [9] and/or production of lymphocyte-inhibiting TGF- $\beta$  [22] by the cells. However, our study clearly shows that the transplantation of mESCs in vivo can result in donor-specific immune recognition and rejection, which leads to immunologic memory. Importantly, post-transplant cell death is accelerated when mESCs are allowed to differentiate before transplantation, a scenario likely to occur in clinical ESC-based transplantation settings in the future. Whether the latter phenomenon is truly a result of increased immunogenicity of the cells, as suggested by their increased expression of MHC antigens (Fig. 1E), or if other factors such as a decreased proliferation rate of differentiated cells play part in this process remains to be evaluated in detail. Nevertheless, the results of this study emphasize that immunologic

rejection of ESCs or ESC derivatives is likely to occur and the need exists for solutions that reduce or eliminate immunologic response following ESC-based transplantation [23]. To develop and test such strategies, there will also be a need for reliable imaging technologies to track and assess behavior of the cells following transplantation. In vivo BLI serves these needs and has the potential to play a prominent role in future ESC-based transplantation research.

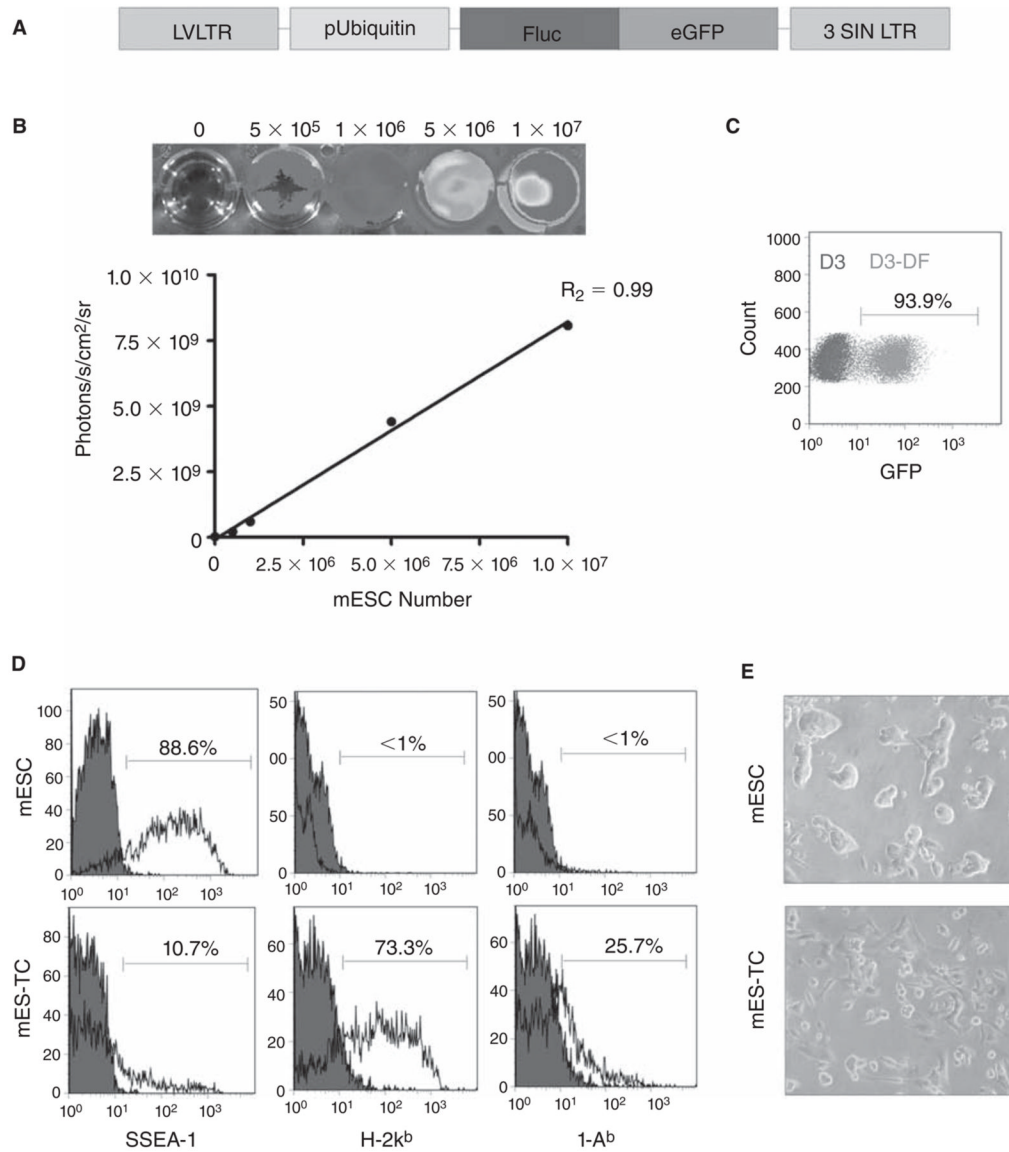
## Acknowledgements

This work was supported by grants from the AHA BGIA, BWF, California Institute of Regenerative Medicine (CIRM) RS1-00322, NHLBI R21HL089027 (J.C.W.), the ISHLT Research Grant (S.S.), and by the ESOT-Astellas Study and Research Grant (R.J.S.). The contents of this publication are solely the responsibility of the authors and do not necessarily represent the official views of CIRM or any other agency of the state of California.

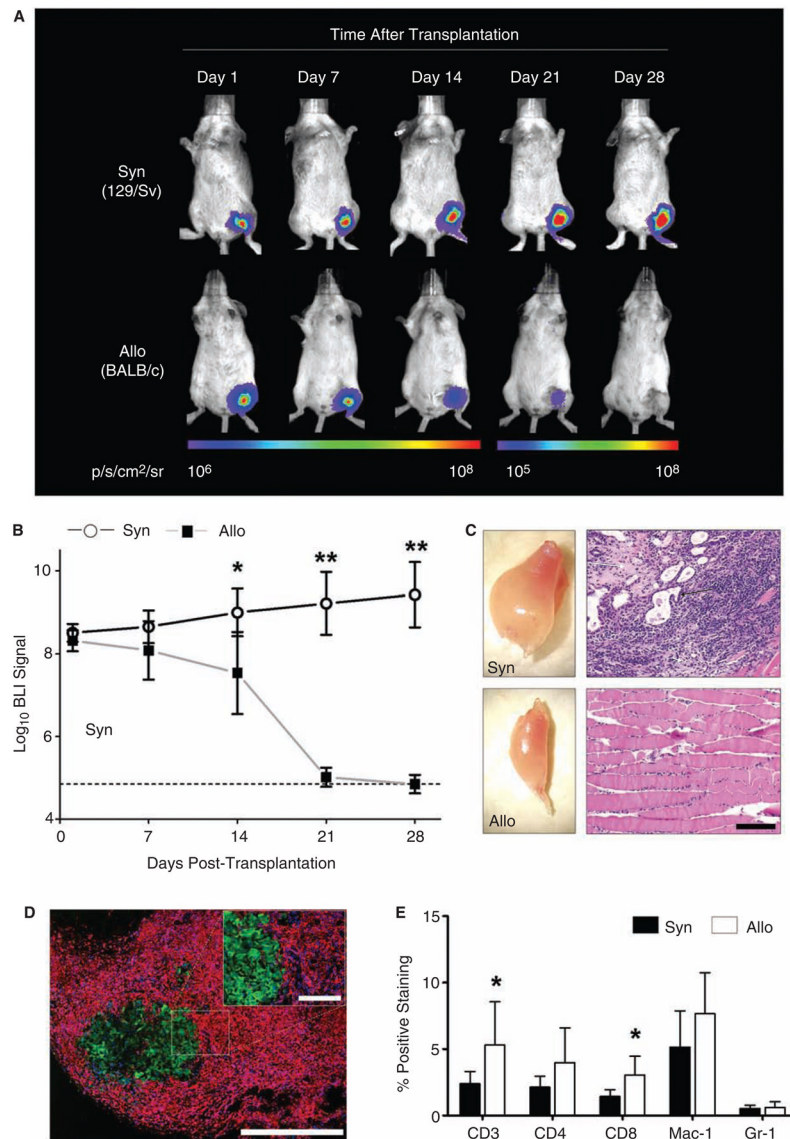
## References

1. Wobus AM, Boheler KR. Embryonic stem cells: prospects for developmental biology and cell therapy. *Physiol Rev* 2005;85:635–678. [PubMed: 15788707]
2. Mummery C, Ward-van Oostwaard D, Doevendans P, Spijker R, van den Brink S, Hassink R, van der Heyden M, Ophof T, Pera M, de la Riviere AB, Passier R, Tertoolen L. Differentiation of human embryonic stem cells to cardiomyocytes: role of coculture with visceral endoderm-like cells. *Circulation* 2003;107:2733–2740. [PubMed: 12742992]
3. Segev H, Fishman B, Ziskind A, Shulman M, Itskovitz-Eldor J. Differentiation of human embryonic stem cells into insulin-producing clusters. *Stem Cells* 2004;22:265–274. [PubMed: 15153604]
4. Perrier AL, Tabar V, Barberi T, Rubio ME, Bruses J, Topf N, Harrison NL, Studer L. Derivation of midbrain dopamine neurons from human embryonic stem cells. *Proc Natl Acad Sci USA* 2004;101:12543–12548. [PubMed: 15310843]
5. Wu DC, Boyd AS, Wood KJ. Embryonic stem cell transplantation: potential applicability in cell replacement therapy and regenerative medicine. *Front Biosci* 2007;12:4525–4535. [PubMed: 17485394]
6. Fandrich F, Dresske B, Bader M, Schulze M. Embryonic stem cells share immune-privileged features relevant for tolerance induction. *J Mol Med* 2002;80:343–350. [PubMed: 12072909]
7. Drukker M, Katz G, Urbach A, Schuldiner M, Markel G, Itskovitz-Eldor J, Reubinoff B, Mandelboim O, Benvenisty N. Characterization of the expression of MHC proteins in human embryonic stem cells. *Proc Natl Acad Sci USA* 2002;99:9864–9869. [PubMed: 12114532]
8. Tian L, Catt JW, O'Neill C, King NJ. Expression of immunoglobulin superfamily cell adhesion molecules on murine embryonic stem cells. *Biol Reprod* 1997;57:561–568. [PubMed: 9282991]
9. Abdullah Z, Saric T, Kashkar H, Baschuk N, Yazdanpanah B, Fleischmann BK, Hescheler J, Kronke M, Utermohlen O. Serpin-6 expression protects embryonic stem cells from lysis by antigen-specific CTL. *J Immunol* 2007;178:3390–3399. [PubMed: 17339433]
10. Li L, Baroja ML, Majumdar A, Chadwick K, Rouleau A, Gallacher L, Ferber I, Lebkowski J, Martin T, Madrenas J, Bhatia M. Human embryonic stem cells possess immune-privileged properties. *Stem Cells* 2004;22:448–456. [PubMed: 15277692]
11. Min JY, Yang Y, Sullivan MF, Ke Q, Converso KL, Chen Y, Morgan JP, Xiao YF. Long-term improvement of cardiac function in rats after infarction by transplantation of embryonic stem cells. *J Thorac Cardiovasc Surg* 2003;125:361–369.
12. Menard C, Hagege AA, Agbulut O, Barro M, Morichetti MC, Brasselet C, Bel A, Messas E, Bissery A, Bruneval P, Desnos M, Puceat M, Menasche P. Transplantation of cardiac-committed mouse embryonic stem cells to infarcted sheep myocardium: a preclinical study. *Lancet* 2005;366:1005–1012. [PubMed: 16168783]
13. Swijnenburg RJ, Tanaka M, Vogel H, Baker J, Kofidis T, Gunawan F, Lebl DR, Caffarelli AD, de Bruin JL, Fedoseyeva EV, Robbins RC. Embryonic stem cell immunogenicity increases upon differentiation after transplantation into ischemic myocardium. *Circulation* 2005;112:1166–172. [PubMed: 16159810]

14. Nussbaum J, Minami E, Laflamme MA, Virag JA, Ware CB, Masino A, Muskheli V, Pabon L, Reinecke H, Murry CE. Transplantation of undifferentiated murine embryonic stem cells in the heart: teratoma formation and immune response. *FASEB J* 2007;21:1345–1357. [PubMed: 17284483]
15. Bonnevie L, Bel A, Sabbah L, Al Attar N, Pradeau P, Weill B, Le Deist F, Bellamy V, Peyrard S, Menard C, Desnos M, Bruneval P, Binder P, Hagege AA, Puceat M, Menasche P. Is xenotransplantation of embryonic stem cells a realistic option? *Transplantation* 2007;83:333–335. [PubMed: 17297408]
16. van der Bogt KE, Swijnenburg RJ, Cao F, Wu JC. Molecular imaging of human embryonic stem cells: keeping an eye on differentiation, tumorigenicity and immunogenicity. *Cell cycle* 2006;5:2748–2752. [PubMed: 17172859]
17. Cao F, Lin S, Xie X, Ray P, Patel M, Zhang X, Drukker M, Dylla SJ, Connolly AJ, Chen X, Weissman IL, Gambhir SS, Wu JC. In vivo visualization of embryonic stem cell survival, proliferation, and migration after cardiac delivery. *Circulation* 2006;113:1005–1014. [PubMed: 16476845]
18. Cao YA, Bachmann MH, Beilhack A, Yang Y, Tanaka M, Swijnenburg RJ, Reeves R, Taylor-Edwards C, Schulz S, Doyle TC, Fathman CG, Robbins RC, Herzenberg LA, Negrin RS, Contag CH. Molecular imaging using labeled donor tissues reveals patterns of engraftment, rejection, and survival in transplantation. *Transplantation* 2005;80:134–139. [PubMed: 16003245]
19. Xie X, Cao F, Sheikh AY, Li Z, Connolly AJ, Pei X, Li RK, Robbins RC, Wu JC. Genetic modification of embryonic stem cells with VEGF enhances cell survival and improves cardiac function. *Cloning and Stem Cells* 2007;9:549–563. [PubMed: 18154515]
20. Cao F, van der Bogt KE, Sadrzadeh A, Xie X, Sheikh AY, Wang H, Connolly AJ, Robbins RC, Wu JC. Spatial and temporal kinetics of teratoma formation from murine embryonic stem cell transplantation. *Stem Cells Dev* 2007;16:883–891. [PubMed: 17896868]
21. Magliocca JF, Held IK, Odorico JS. Undifferentiated murine embryonic stem cells cannot induce portal tolerance but may possess immune privilege secondary to reduced major histocompatibility complex antigen expression. *Stem Cells and Dev* 2006;15:707–717.
22. Koch CA, Geraldles P, Platt JL. Immunosuppression by embryonic stem cells. *Stem Cells* 2008;26:89–98. [PubMed: 17962705]
23. Drukker M. Immunogenicity of human embryonic stem cells: can we achieve tolerance? *Springer Semin Immun* 2004;26:201–213.



**FIG. 1.** Characterization of the double fusion (DF) firefly luciferase (Fluc) and enhanced green fluorescent protein (eGFP) transduced D3 murine embryonic stem cells (mESCs). **(A)** Schema of the DF reporter gene containing Fluc and eGFP driven by an ubiquitin promoter. **(B)** Stably transduced mESCs show a robust correlation between cell number and reporter gene activity. BLI of a 24-well plate containing increasing numbers of mESCs are shown above the corresponding graph depicting correlation between cell number and Fluc activity. **(C)** Flow cytometric analysis of transduced mESCs (D3-DF) shows robust expression of eGFP following transduction with the DF reporter gene, as compared to nontransduced mESCs (D3). **(D)** Flow cytometric analysis of undifferentiated mESCs shows robust expression of pluripotency marker SSEA-1, but minimal expression of MHC-I (H-2k<sup>b</sup>) or MHC-II (I-A<sup>b</sup>) antigens. In contrast, cells isolated from a 6-week-old teratoma derived from mESCs (mES-TCs) express low amounts of SSEA-1 but significant levels of MHC-I and MHC-II antigens. Filled histograms represent isotype control antibodies. **(E)** Phase-contrast images of undifferentiated mESCs and mES-TCs cultured in vitro.

**FIG. 2.**

In vivo bioluminescent imaging (BLI) of transplanted mESCs. (A) Representative BLI images of animals following intramuscular (gastrocnemius muscle) transplantation of mESCs show a decrease in BLI signal in allogeneic animals (BALB/c), as opposed to syngeneic (129/Sv) mice, reaching background levels between post-transplant Days 21 and 28. Color scale bar values are in photons/sec/cm<sup>2</sup>/steradian (p/s/cm<sup>2</sup>/sr). (B) Graphical representation of longitudinal BLI after mESC transplantation into syngeneic (129/Sv, *n* = 8) and allogeneic (BALB/c, *n* = 8) mouse strains. Note that in allogeneic recipients, BLI signals decrease to background levels over the course of 28 days, whereas BLI signals in the syngeneic recipients increase over time, suggesting mESC proliferation. Data points represent mean ± SD; \**p* < 0.01, \*\**p* < 0.001 (by *t*-test). Dotted line = background BLI signal. (C) Ex vivo images of harvested muscles (left panels) show intramuscular tumors in syngeneic, as opposed to allogeneic muscles. Corresponding H&E-stained tissue sections (right panels) show presence of teratoma in syngeneic muscles, whereas no signs of teratoma formation are observed in allogeneic muscles. Black arrow: Osteoid differentiation (mesoderm); White arrow: glandular differentiation

(endoderm); Black arrow head: neural differentiation (ectoderm). Scale bars: 100  $\mu\text{m}$ . **(D)** Immunofluorescent staining of allogeneic transplants reveals severe infiltration of CD45<sup>+</sup> cells (red) surrounding eGFP<sup>+</sup> mESCs (green). Nuclear staining was performed with 4,6-diamidino-2-phenylindole (DAPI, blue). Scale bars: 100  $\mu\text{m}$ . **(E)** To quantify subpopulations of graft infiltrating inflammatory cells, flow cytometry analysis of enzymatically digested muscles was performed at Day 10 following transplant. Graft infiltration of CD3<sup>+</sup> (T-cells), CD4<sup>+</sup> (T-helper cells), CD8<sup>+</sup> (cytotoxic T-cells), Mac-1<sup>+</sup>Gr-1<sup>-</sup> (macrophages), and Mac-1<sup>+</sup>Gr-1<sup>+</sup> (neutrophils) was observed. Note that CD3<sup>+</sup> and CD8<sup>+</sup> cells infiltrated the allogeneic grafts at a significantly higher rate than the syngeneic grafts ( $n = 8$  per group). Bars represent mean  $\pm$  SD; \* $p < 0.05$  (by  $t$ -test).



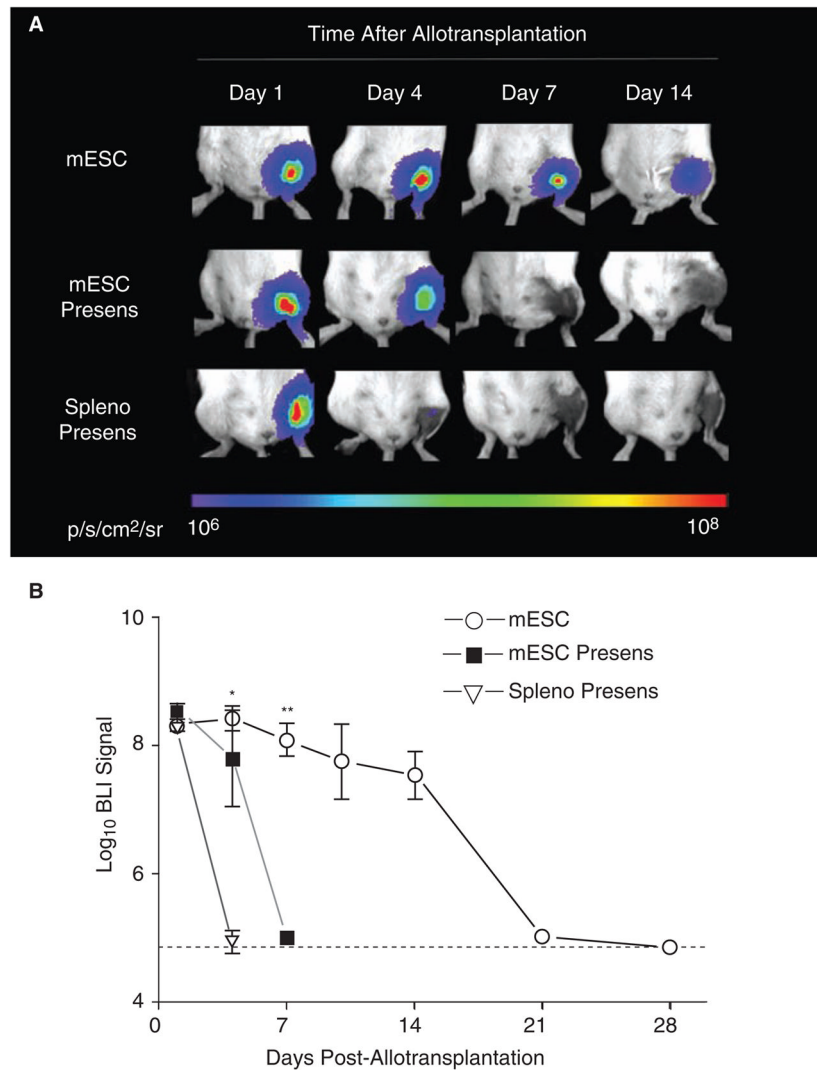


**FIG. 3.** Accelerated rejection following presensitization of the host. **(A)** Representative BLI images of animals following intramuscular allotransplantation of mESCs show an accelerated decrease in BLI signal in animals that were presensitized with both nontransduced mESCs (mESC presens) or irradiated 129/Sv splenocytes (spleno presens) as compared to naïve allogeneic mESC recipients. Color scale bar values are in p/s/cm<sup>2</sup>/sr. **(B)** Graphical representation of BLI of mESC survival in the three groups ( $n = 4-8$  per group). Data points represent mean  $\pm$  SEM; \* $p < 0.001$  mESC vs. spleno presens, \*\* $p < 0.001$  mESC versus mESC presens (by ANOVA). Dotted line = background BLI signal.

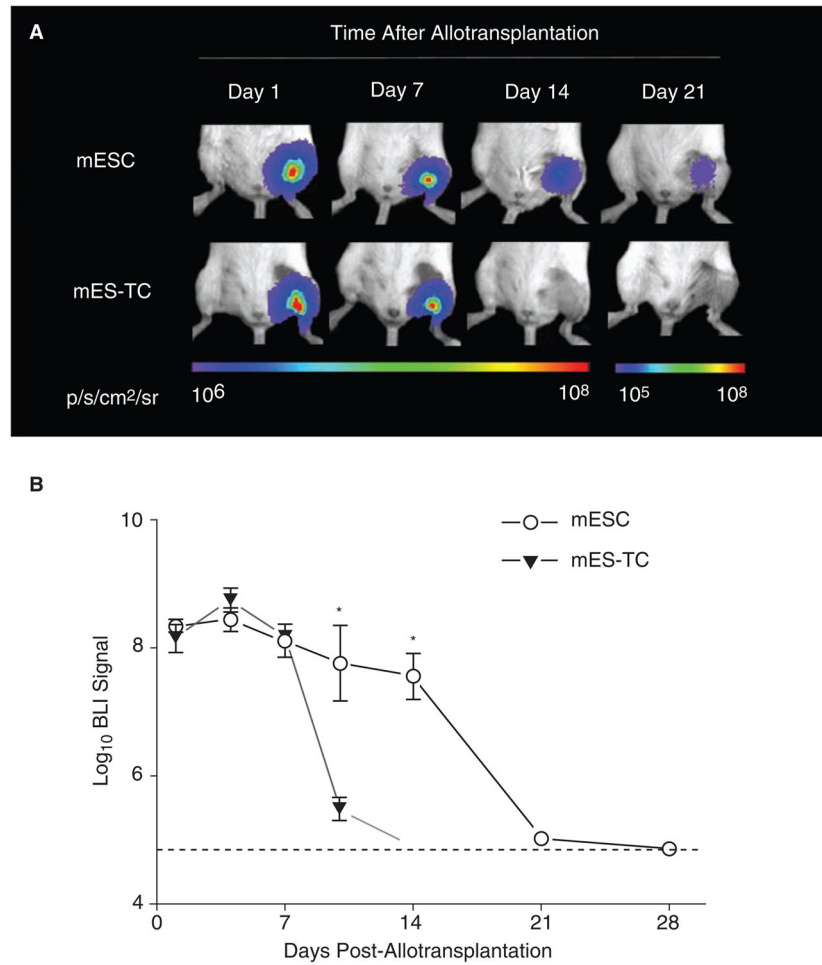


**FIG. 4.** Impaired survival capacity of differentiated mESCs as compared to undifferentiated mESCs following allotransplantation. **(A)** Representative BLI images of animals following intramuscular allotransplantation of mESCs or mES-TCs. Clearly, BLI signal in the mES-TC-transplanted animals decreased more rapidly as compared to mESC-transplanted animals, reaching background levels at Day 14. Color scale bar values are in p/s/cm<sup>2</sup>/sr. **(B)** Graphical representation of BLI of mESC survival in the two groups ( $n = 5-8$  per group). Data points represent mean  $\pm$  SEM; \* $p < 0.01$  (by  $t$ -test). Dotted line = background BLI signal.